

Deletion of *ETS-1*, a gene in the Jacobsen syndrome critical region, causes ventricular septal defects and abnormal ventricular morphology in mice

Maoqing Ye¹, Chris Coldren², Xingqun Liang³, Teresa Mattina^{4,5}, Elizabeth Goldmuntz⁶, D. Woodrow Benson⁷, Dunbar Ivy⁸, M.B. Perryman⁹, Lee Ann Garrett-Sinha¹⁰ and Paul Grossfeld^{1,*}

¹Division of Pediatric Cardiology, Department of Pediatrics/Rady Children's Hospital of San Diego and ²Division of Pulmonary Medicine, UCHSC, CO, USA, ³Department of Medicine, UCSD, CA, USA, ⁴Department of Medical Genetics and ⁵Department of Pediatrics, University of Catania, Italy, ⁶Division of Pediatric Cardiology, Children's Hospital of Philadelphia, PA, USA, ⁷Division of Pediatric Cardiology, Cincinnati Children's Hospital, OH, USA, ⁸Division of Pediatric Cardiology, The Children's Hospital of Denver, CO, USA, ⁹Sanford Research, University of South Dakota, Sanford Health, SD, USA and ¹⁰Department of Biological Chemistry, SUNY-Buffalo, NY, USA

Received September 23, 2009; Revised November 17, 2009; Accepted November 24, 2009

Congenital heart defects comprise the most common form of major birth defects, affecting 0.7% of all newborn infants. Jacobsen syndrome (11q-) is a rare chromosomal disorder caused by deletions in distal 11q. We have previously determined that a wide spectrum of the most common congenital heart defects occur in 11q-, including an unprecedented high frequency of hypoplastic left heart syndrome (HLHS). We identified an ~7 Mb 'cardiac critical region' in distal 11q that contains a putative causative gene(s) for congenital heart disease. In this study, we utilized chromosomal microarray mapping to characterize three patients with 11q- and congenital heart defects that carry interstitial deletions overlapping the 7 Mb cardiac critical region. We propose that this 1.2 Mb region of overlap harbors a gene(s) that causes at least a subset of the congenital heart defects that occur in 11q-. We demonstrate that one gene in this region, *ETS-1* (a member of the *ETS* family of transcription factors), is expressed in the endocardium and neural crest during early mouse heart development. Gene-targeted deletion of *ETS-1* in mice in a C57/B6 background causes, with high penetrance, large membranous ventricular septal defects and a bifid cardiac apex, and less frequently a non-apex-forming left ventricle (one of the hallmarks of HLHS). Our results implicate an important role for the *ETS-1* transcription factor in mammalian heart development and should provide important insights into some of the most common forms of congenital heart disease.

INTRODUCTION

The 11q terminal deletion disorder (11q-), OMIM 147791, is a rare chromosomal disorder caused by deletions in distal 11q (1–4). Deletion sizes vary in size from 5 to 16 Mb. Most of the deletions that have been characterized in 11q- patients using molecular methods are terminal, extending to the telomere. We previously performed a prospective genotype/

phenotype study on 110 11q- patients with terminal 11q deletions. We defined 'critical regions' for 14 clinical phenotypes, consistent with a contiguous gene model for the constellation of clinical problems that occur in 11q- (4).

Fifty-six percent of 11q- patients has clinically significant congenital heart defects (Table 1) that require medical and/or surgical intervention, and there is no correlation between deletion size and the presence, or type, of congenital heart

*To whom correspondence should be addressed at: Division of Pediatric Cardiology, UCSD School of Medicine, 3030 Children's Way, MC 5004, San Diego, CA 92123, USA. Tel: +1 8589665855; Fax: +1 8585717903; Email: pgrossfeld@ucsd.edu or pgmd@aol.com

Table 1. Congenital heart defects in 11q-

Flow defects	Miscellaneous defects
Hypoplastic left heart syndrome	Secundum atrial septal defects
Shone's complex	Double outlet right ventricle
Coarctation of the aorta	Aberrant right subclavian artery
Bicuspid aortic valve	Complete atrioventricular canal defect
Aortic valve stenosis	D-transposition of the great arteries
Mitral valve stenosis	Dextrocardia
Membranous ventricular septal defect	Left-sided superior vena cava
	Tricuspid atresia
	Type B interruption of the aortic arch
	Truncus arteriosus
	Pulmonary valve atresia
	Total anomalous pulmonary venous return

defect. Of the 56% of patients with congenital heart disease, two-thirds have cardiac flow defects, which are defined specifically as ventricular septal defects (~40% of 11q- patients with congenital heart disease) and left-sided obstructive lesions, all of which are caused by decreased blood flow through the heart during development. Remarkably, we found that hypoplastic left heart syndrome (HLHS), the most severe cardiac flow defect, occurs in ~5–10% of all 11q- patients, higher than for any other known chromosomal disorder. In addition to cardiac flow defects, defects affecting most of the other structures of the heart also occur in 11q- patients. Hence, understanding the genetic basis of the congenital heart defects in 11q- could provide insight into the pathogenesis of many of the most common and severe forms of congenital heart disease.

In this study, we refine the cardiac critical region in distal 11q based on a region of overlap between patients with terminal and, more recently identified, interstitial deletions in distal 11q. The smallest region of overlap for HLHS is 1.2 Mb and contains only six annotated genes. We identify one gene in this region, *ETS-1*, as a candidate gene for causing congenital heart defects in 11q-.

ETS-1 is a member of the *ETS* family of transcription factors. This family of transcription factors, including *ETS-1*, has important roles in a wide range of biological functions, including the regulation of cellular growth and differentiation as well as in organ development, hematopoiesis (5–7), lymphocyte development (8–14), vascular development and angiogenesis (15), and in the regulation of vascular inflammation and remodeling (16). Although neonatal lethality, of an unknown etiology, has been described (9), none of these studies included comprehensive cardiac phenotyping to determine whether the loss of *ETS-1* causes structural heart defects.

Recent studies have implicated an important role for *ETS-1* in heart development in non-mammalian species, including chordates, fruitflies and chicks (17–19). For example, Davidson *et al.* (17) have demonstrated that the inhibition of the ortholog of *ETS-1* in the chordate *Ciona intestinalis* is essential for heart development, and that the ectopic expression in a skeletal muscle progenitor cell gives rise to an ectopically located beating cardiac chamber.

The role of *ETS-1* in mammalian heart development, and in the causation of human congenital heart defects, is unknown.

We demonstrate that deletion of *ETS-1* in mice recapitulates some of the most common congenital heart defects in 11q-, including membranous ventricular septal defects and impaired ventricular development. The results of these studies implicate a critical role for *ETS-1* during mammalian heart development and in the pathogenesis of some forms of human congenital heart disease.

RESULTS

Deletion mapping and refinement of the cardiac critical region

Initial karyotype analysis identified the presence of deletions in distal 11q in over 150 previously identified patients that were subsequently selected to undergo higher resolution mapping by either FISH (4) or chromosomal microarray mapping (CMM). One patient (JS22) with HLHS had the smallest terminal deletion of any of the patients from our original cohort of 110 patients (~7 Mb), originally mapped by FISH. Three patients with congenital heart defects had interstitial deletions in distal 11q, originally detected by the karyotype analysis: double outlet right ventricle (JS2), HLHS (JS4) and an atrial septal defect (JS14). The results of the CMM mapping are shown in Figure 1 and Table 2. The smallest terminal deletion was 7 Mb. The patients with interstitial deletions overlapped the 7 Mb terminal region by 3.2 Mb (JS2), 1.2 Mb (JS4) and 0.8 Mb (JS22). Consequently, the refined HLHS critical region is 1.2 Mb. As shown in Figure 1, this region contains only six annotated genes: *ETS-1*, *FLI-1*, *KCNJ1*, *KCNJ5*, *P53AIP1* and *RICS*. Five of these genes (*ETS-1*, *FLI-1*, *KCNJ-1*, *KCNJ5* and *RICS*) have been deleted in the mouse and, in addition to *ETS-1*, none of them are reported to have structural heart defects (9,20–24). We also performed mutation analysis by direct DNA sequencing of the *P53AIP1* gene in 200 patients with isolated HLHS, and no disease-causing DNA sequence changes were identified (data not shown), suggesting that the mutations in *p53AIP1* do not cause congenital heart defects (an analysis for microdeletions spanning *p53AIP1* was not performed). The smallest region of overlap for any kind of congenital heart defect contains only two of these genes, *ETS-1* and *FLI-1*. Initially, we analyzed *FLI-1* mutant mice, including ED10.5–12.5 hearts from a *FLI-1* null mutant strain and neonatal hearts from a hypomorphic *FLI-1* mutant strain, both in a C57/B6 pure background (kindly provided by Dr Dennis Watson, MUSC). No structural heart defects were detected (data not shown). Because of the absence of heart defects in *FLI-1* mutant mice, combined with the known roles of *ETS-1* in cardiovascular development, we propose *ETS-1* as a candidate gene for causing at least a subset of the heart defects in 11q-.

Expression of *ETS-1* during murine heart development

To determine the pattern of expression of *ETS-1* in the developing mouse heart, *in situ* hybridization was performed in combination with immunohistochemistry and immunofluorescence using a PECAM (CD31, an endothelial marker) antibody, and analysis of Wnt1-Cre; ROSA26 LacZ mice (a neural crest cell indicator strain). As shown in Figure 2A–J,

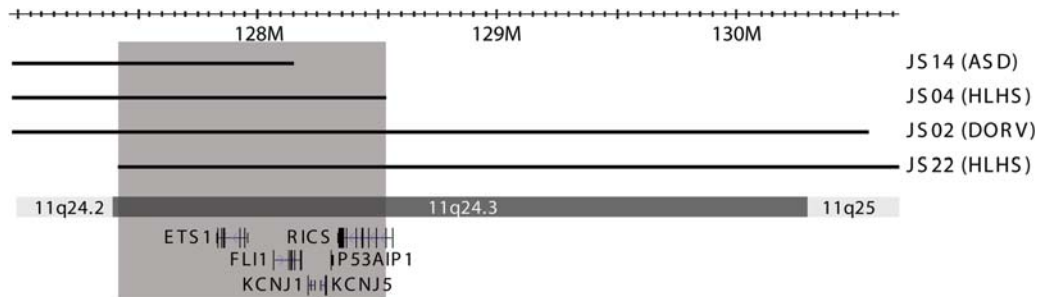


Figure 1. Refined critical region in distal 11q. The new region is defined by the region of overlap between the previously defined ~7 Mb terminal deletion (JS22), and that of the three patients with congenital heart defects with interstitial deletions in distal 11q.

Table 2. Breakpoints of patients with 11q deletions

Subject	Last diploid	First haploid	Last haploid	First diploid
JS02-DORV	121842621	121867740	130562600	130569534
JS04-HLHS ^a	121366328	121399235	128523204	128559769
JS14-ASD	120436015	120476074	128147958	128186180
JS22-HLHS	127408912	127437820	Terminal	

^aThis patient was found to have a small second interstitial deletion centromeric to the original cardiac critical region (breakpoints from 119 110 690 to 119 996 189).

ETS-1 expression is first detected in the endothelial tissue lining the primitive heart tube in ED8 embryos, and is localized to the endocardium of the atrium and ventricle in ED8.75 hearts. The expression of *ETS-1* in the endothelium was confirmed by comparison to that of *PECAM*.

As shown in Figure 3A, *ETS-1* is expressed robustly throughout the vascular endothelium by ED9.5, consistent with the results published by Maroulakous *et al.* (25). *ETS-1* expression was also detected in the endothelium of the atrium, atrioventricular canal, ventricles and outflow tract (Fig. 3B–F). In addition, *ETS-1* expression was detected in the neural crest by comparing the expression pattern to *Wnt1-Cre; ROSA26 LacZ* mice (26) (Fig. 3G–I). By ED13.5, *ETS-1* expression was detected in the region of the developing membranous septum (Fig. 4A) as well as in the endocardium lining the myocardial trabeculations (Fig. 4B and C).

Expression of *ETS-1* in cultured neural crest cells derived from ED8.5 neural crest explanted tissue

To confirm expression of *ETS-1* in neural crest cells, immunofluorescence studies were performed using *ETS-1* and *SOX-10* antibodies (as a marker for neural crest) on neural crest cells cultured from neural crest explants derived from ED8.5 embryos. As shown in Figure 3J–M, there was robust and specific expression of *ETS-1* in the nucleus of ED8.5 neural crest cells, confirming the immunohistochemistry results.

Cardiac phenotyping of *ETS-1*-deleted mice

Histopathologic analysis was performed on a total of 48 ED15.5–17.5 mice derived from five litters. The results are

shown in Table 3 and Figure 5. All nine homozygous *ETS-1* deletion mice had large membranous ventricular septal defects (Fig. 5D and F). Six of these had an abnormal-appearing left ventricular morphology, characterized by a bifid cardiac apex, and two of these had a non-apex-forming left ventricle (Fig. 5F). The remainder of the cardiac anatomy, including the valves, aorta and venous structures was normal. One heterozygous mouse had a small ventricular septal defect. The hearts from all 16 wild-type embryos had normal structure. The number of homozygous *ETS-1* null embryos that we identified is less than predicted for Mendelian inheritance, suggestive of embryonic lethality and the possibility of a more severe cardiac phenotype that we would not have identified. This is most likely due to the relatively small number of embryos that we analyzed, given that previous studies of *ETS-1* knockout mice have not described embryonic lethality (8–14,16).

DISCUSSION

We have previously performed a comprehensive genotype/phenotype analysis on 110 patients with 11q- (Jacobsen syndrome). We determined that many of the most common congenital heart defects that occur in the general population occur in 11q-. Fifty-six percent of 11q- patients had congenital heart disease, and there was no correlation between the size of deletion and the presence of, or type of, congenital heart defect. In that study, we defined a 7 Mb cardiac ‘critical region’ that contains a putative disease-causing gene(s) for congenital heart defects. This region contains over 40 annotated genes.

In the present study, we performed high resolution chromosomal microarray mapping on three recently identified patients with the 11q- clinical phenotype, including congenital heart defects, that have interstitial deletions overlapping the previously defined 7 Mb cardiac critical region. Based on our human genetics data, previous functional studies and the absence of heart defects in *FLI-1* mutant mice, we propose *ETS-1* as a candidate gene for causing at least a subset of the congenital heart defects that occur in 11q-.

Recently, Tyson *et al.* (27) proposed a potential 1.57 Mb cardiac critical region in distal 11q that is telomeric to *ETS-1* and *FLI-1*. This hypothesis was based on two patients with interstitial deletions in distal 11q that did not have congenital heart disease, but overlapped the interstitial deletion of a

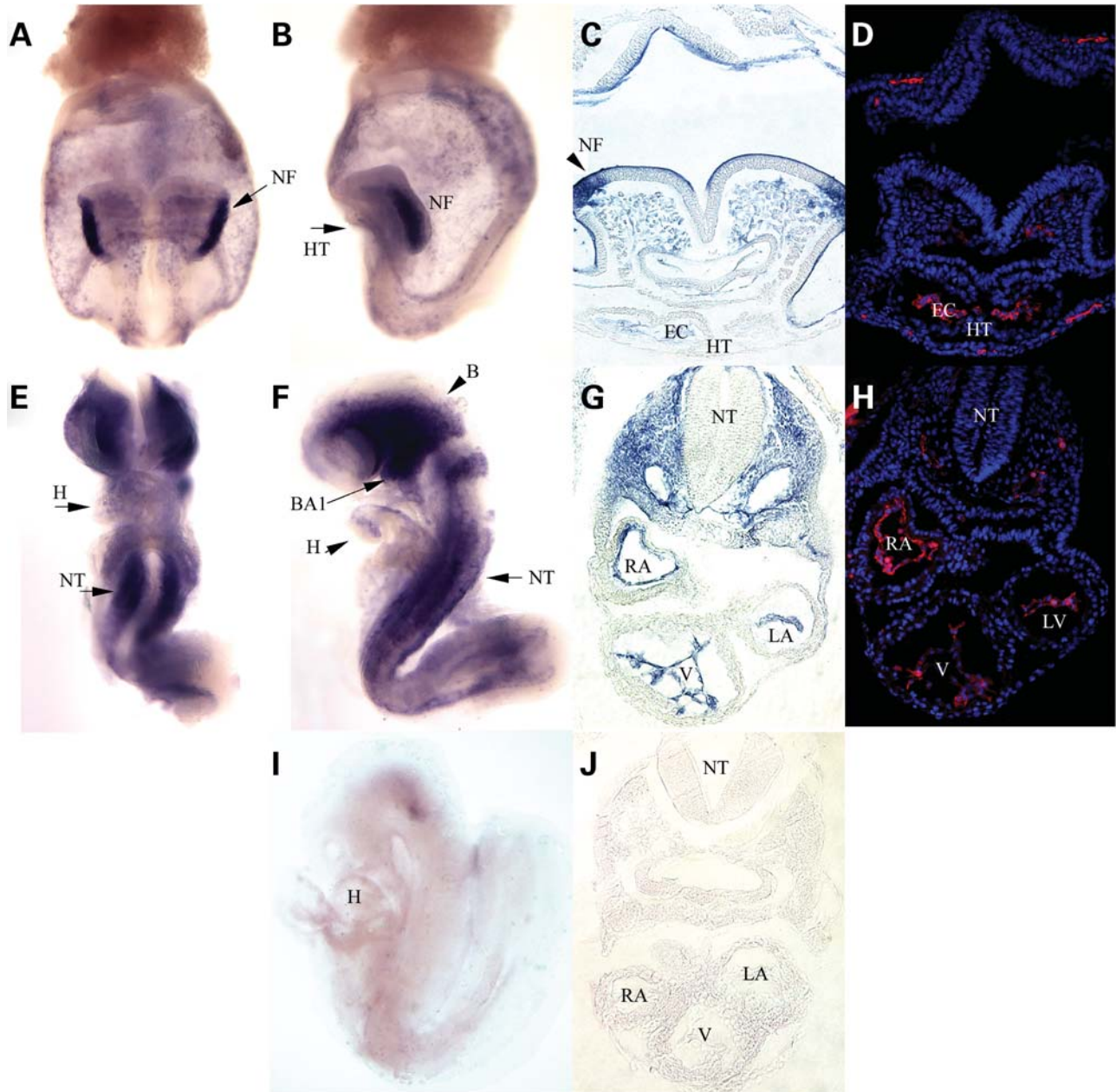


Figure 2. Early expression of *ETS-1* in the developing mouse heart: ED8 *in situ* hybridization showing whole mount (A and B), coronal section and staining of endothelium using PECAM (CD31) antibody (C and D). ED8.75 *in situ* hybridization showing whole mount (E and F), coronal section (G), PECAM staining (H) and negative control for *in situ* using an *ETS-1* sense probe (I and J). NF, neural fold; HT, heart tube; EC, endocardial cell; NT, neural tube; H, heart; BA1, first branchial arch; RA, right side of common atrium; LA, left side of common atrium; V, ventricle.

patient with double outlet right ventricle that we described previously (JS2) (28). Given the incomplete penetrance for congenital heart disease in 11q-, we propose that only deletions from patients with congenital heart defects should define the cardiac critical region, as we describe in the present study. In addition, Bernaciak *et al.* (29) recently described four patients with some features of 11q- that have the smallest 11q terminal deletion reported to date, 5 Mb. These deletions overlapped the critical region proposed by Tyson *et al.* None of these patients had congenital heart defects, consistent with our model for a more centromeric

location for the cardiac critical region. Our refined cardiac critical region also does not contain *JAM-3*, a gene proposed previously as a candidate gene for causing heart defects in 11q- (30). Consistent with this, we have recently demonstrated that *JAM-C* knockout mice do not have structural heart defects (31).

Phenotypic analysis of gene-targeted *ETS-1* knockout mice demonstrated that deletion of *ETS-1* in a pure C57/B6 background caused, with high penetrance, large membranous ventricular septal defects and frequently an abnormal-appearing ventricular morphology characterized by a bifid apex.

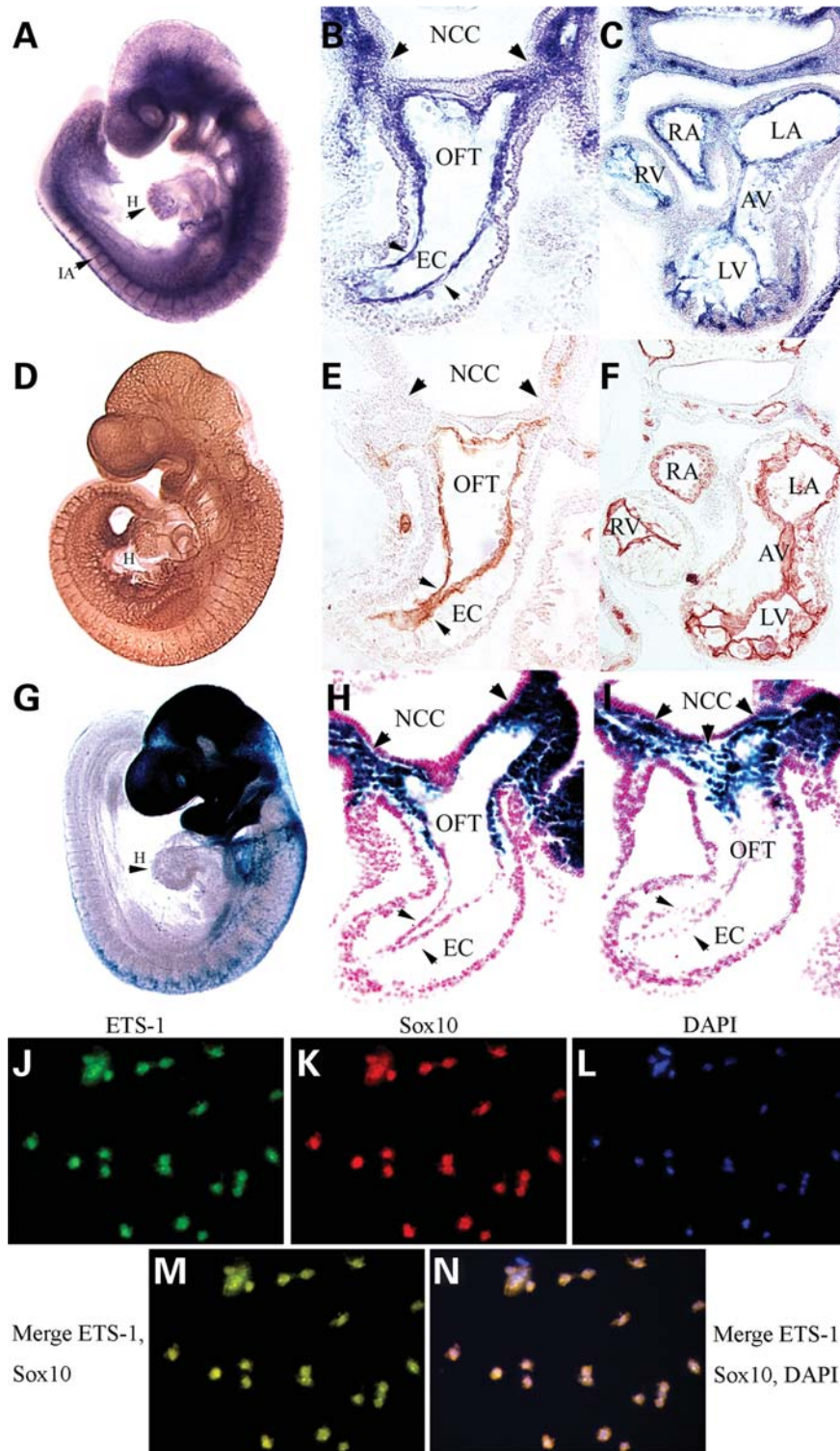


Figure 3. Expression of ETS-1 in the heart in ED9.5 embryos: *in situ* hybridizations are shown in (A) (whole mount), and in sections: (B) (anterior coronal section) and (C) (posterior coronal section). Immunohistochemistry indicating endothelial expression using a PECAM (CD31) antibody is shown in (D) (whole mount), and in sections: (E) (anterior coronal) and (F) (posterior coronal). LacZ staining of neural crest using a Wnt1-Cre; ROSA26 LacZ indicator strain is shown in (G) (whole mount), (H) (anterior coronal) and (I) (posterior coronal). Immunofluorescence studies on cultured neural crest cells derived from ED8.5 neural crest explanted tissue: ETS-1 antibody (J); Sox10 antibody (K), DAPI staining (L); Merge of ETS-1 and Sox10 (M); Merge of ETS-1, Sox10 and DAPI (N). RA, right side of common atrium; LA, left side of common atrium; AV, atrioventricular canal; RV, right side of common ventricle; LV, left side of common ventricle; OFT, outflow tract; NCC, neural crest cell; EC, endothelial cell.

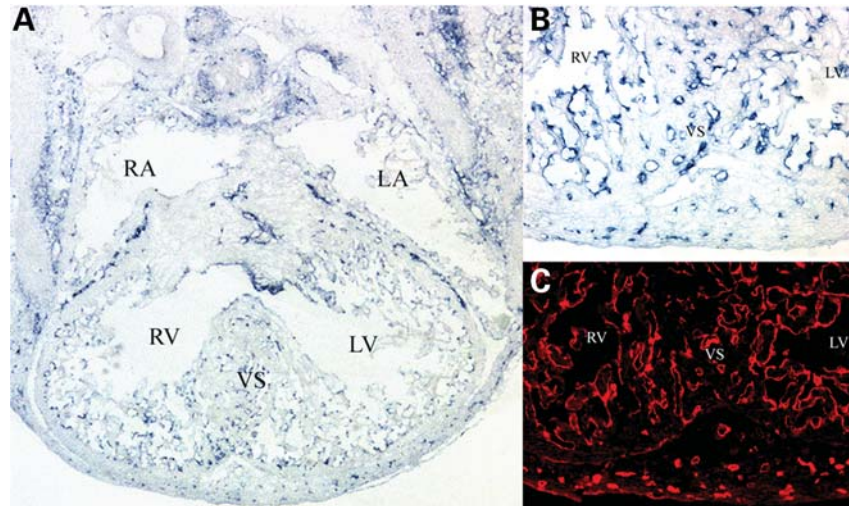


Figure 4. *In situ* hybridization showing expression of *ETS-1* in the region of the developing membranous interventricular septum in an ED13.5 heart (A). Higher magnification of myocardial trabeculations from an ED13.5 heart showing expression of *ETS-1* in the endocardium: *in situ* hybridization (B) and immunofluorescence using an antibody to PECAM (C). RA, right atrium; LA, left atrium; RV, right ventricle; LV, left ventricle; VS, interventricular septum. *ETS-1* expression is also detected in the endocardium of the semilunar and atrioventricular valves by ED13.5 (data not shown).

Table 3. Cardiac phenotypes of *ETS-1* mice

Genotype	No.	VSD	Bifid apex	Non-apex LV
+/+	16	0	0	0
+/-	23	1	0	0
-/-	9	9	6	2

The appearance of a bifid apex in the *ETS-1* null mice has been described previously as a normal transient finding during early murine and human heart development. However, persistence of a bifid apex through later stages of heart development is indicative of an arrest of normal ventricular development (32,33). In addition, a subset of the *ETS-1* null mice (2/9) had a non-apex-forming left ventricle, one of the hallmarks of HLHS, although the other structures usually affected in HLHS were normal. Taken together, these results implicate a role for *ETS-1* in ventricular development. The presence of a cardiac phenotype was dependent on the genetic background, paralleling what occurs in 11q- patients.

High *et al.* (34) have demonstrated that impaired differentiation of the neural crest during cardiac development in mice causes ventricular septal defects. Consistent with this model, our studies indicate that *ETS-1* is expressed in the neural crest, and suggest that the loss of *ETS-1* in the neural crest causes ventricular septal defects. In further support of a role for *ETS-1* in the neural crest during development, we have observed hypopigmentation in the fur of *ETS-1* heterozygotes (Supplementary Material, Fig. S1). This is similar to what has been described in mice carrying the *splotch* mutation of *PAX-3*, a gene that is essential for neural crest function during development (35).

The role of *ETS-1* in the endocardium during heart development is unclear. Because *ETS-1* expression was not detected in the myocardium, one possibility is that *ETS-1* is required in the endocardium for normal myocardial development

through a non-cell autonomous mechanism. Alternatively, it is possible that the loss of *ETS-1* in the vascular endothelium causes congenital heart defects secondary to impaired hemodynamics during heart development.

In summary, our studies implicate an important role for *ETS-1* in human heart development and in the etiology of some of the most common congenital heart defects. Future studies will be aimed at defining the genetic pathways and developmental lineages involving *ETS-1* in normal heart development, and how decreased *ETS-1* function causes human congenital heart defects.

MATERIALS AND METHODS

Patient recruitment

Patients were identified through the 11q Research and Resource group (www.11qusa.org) as well as through physician referrals. Studies were performed in compliance with a UCSD Institutional Review Board-approved protocol. Patients JS4 and JS2 have been described previously (4).

Chromosomal microarray mapping (CMM)

High resolution mapping of the deletion breakpoints was performed using the Affymetrix 500K SNP platform, as described previously (37) using total genomic isolated DNA isolated from fresh whole blood. The Affymetrix Human Mapping 500 K SNP array set consists of two arrays: the 250 K Nsp array and the 250 K Sty array. These assays were performed by the University of Colorado Cancer Center microarray core facility following the protocol developed by the manufacturer. In short, 250 ng of genomic DNA is digested with 10 units of NspI or StyI (New England Biolabs, Beverly, MA, USA) for 2 h at 37°C. Specific adaptors are ligated onto the digested ends with T4 DNA Ligase for 2 h at 16°C. After dilution with water, samples were subjected to PCR using

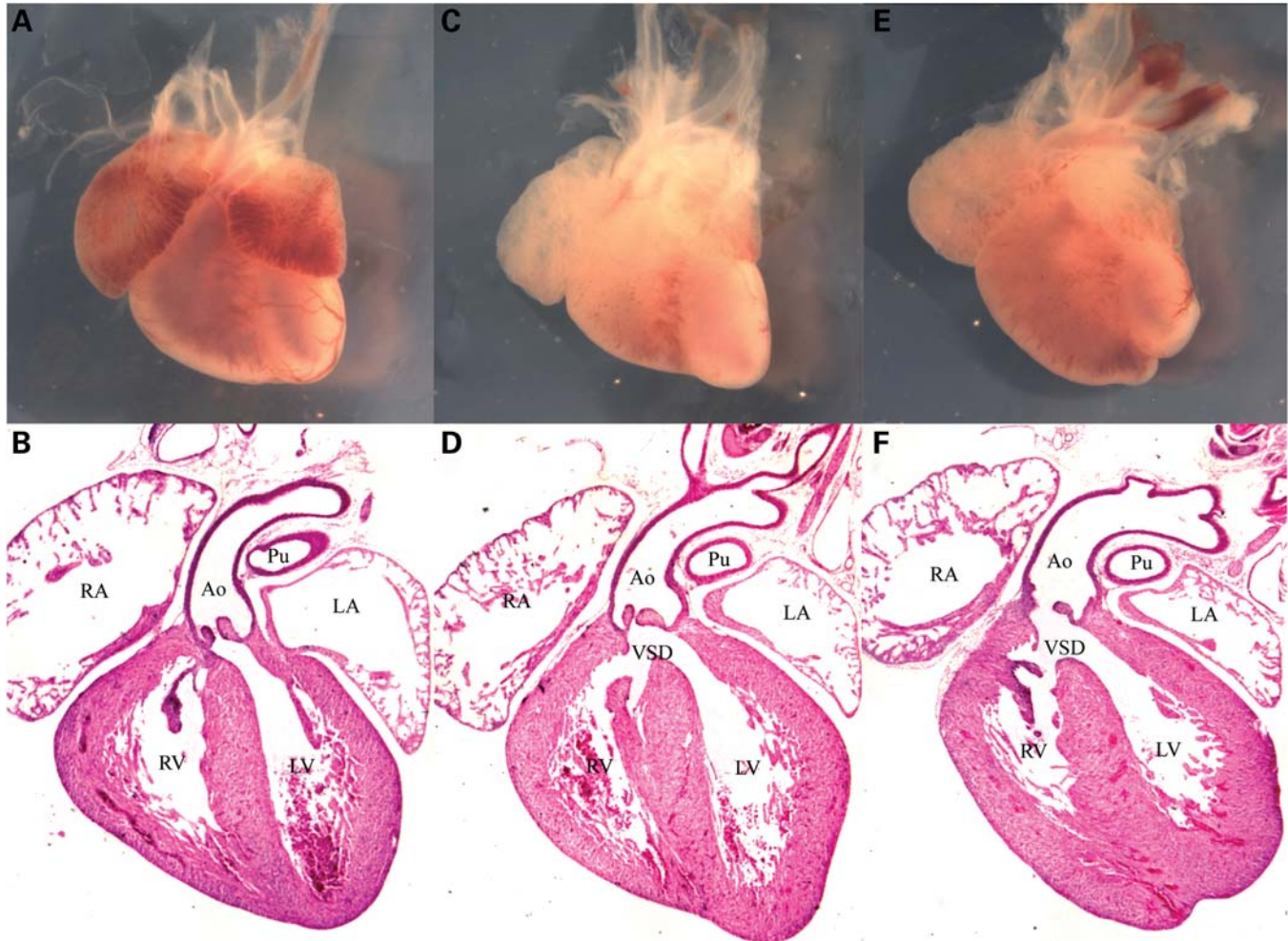


Figure 5. Large membranous ventricular septal defect in ED16.5 *ETS*^{-/-} embryos, indicated by arrowhead [wild-type is shown in (A) and (B); two mutant hearts are shown in panels (C)–(F)]. RA, right atrium; LA, left atrium; RV, right ventricle; LV, left ventricle; Pu, pulmonary artery; Ao, aorta; VSD, ventricular septal defect.

primers specific to the adaptor sequence with the following amplification parameters: 95°C for 3 min (initial denaturation), 95°C for 20 s, 59°C for 15 s, 72°C for 15 s for a total of 35 cycles, followed by 72°C for 7 min (final extension). PCR products were purified and fragmented using 0.24 units of DNase I at 37°C for 30 min. The fragmented DNA was subsequently end-labeled with biotin using 100 units of terminal deoxynucleotidyl transferase at 37°C for 2 h. Labeled DNA was then hybridized onto the corresponding 250 K Mapping Array at 48°C for 16–18 h at 60 rpm. The hybridized array was washed, stained and scanned according to the manufacturer's instructions. Identification of genomic segments with altered copy number data was performed using hidden Markov models (HMM), as implemented in the software package CNAT4.0 (Affymetrix, Santa Clara, CA, USA). Regions of chromosome 11 that were identified as monosomic were validated using the SNP array genotype data. Whereas the genome-wide heterozygosity rate was 27–28%, heterozygous calls were less common in the monosomic segments (7–9%). Genomic segments exhibiting loss of heterozygosity (LOH) were identified using HMM, and these regions were

identical to the monosomic segments. These results were compiled and examined in genomic context (NCBI Build 36.1) using the UCSC genome browser.

In situ hybridization

In situ hybridization using the whole mount embryos was performed as described previously (38). Embryos were hybridized with digoxigenin-labeled RNA probes. Hybridization was detected with anti-digoxigenin antibody coupled to alkaline phosphatase. The probes used were: forward: 5'-CGG CCG TCG ATC TCA AGC CGA CTC; reverse: 3'-CTG CCA CAG CTG GAT CGG CCC AC.

Neural crest cultures

Neural crest cell cultures were isolated as described (38). Briefly, embryos were collected at E8.5 (4 to 10 somites). The portion of neural tube between the otic placode and the third somite was microdissected out, transected and cultured in fibronectin-coated 2-well slide chambers (NUNC,

Lab-Tek™ Chamber Slide™ System) containing high-glucose DME and 10% fetal bovine serum. Cultures were maintained for 48 h at 37°C with 5% CO₂, and then neural tube explant was removed and discarded. Neural crest cell outgrowths attached to the culture were used for immunofluorescence studies.

Immunofluorescence studies

Immunofluorescence staining was performed as described (38). Briefly, 8 μm cryo-sections were incubated with primary antibodies overnight at 4°C. The following primary antibodies were used: PECAM (1:100; Vector laboratories, VP-C344), ETS-1 (1:100; Santa Cruz Biotechnology, sc-350), Sox10 (gift of M. Wegner). After washing with 0.25% TritonX-100 in PBS, sections were incubated with biotinylated secondary (Vector) antibodies for 2 h.

Whole mount PECAM immunohistochemistry staining was performed as described previously (38). A 1:100 dilution of rat antibodies against mouse PECAM (Vector laboratories) in PBS, 1.5% milk and 0.2% triton-100 and a 1:500 dilution of HRP-conjugated affinity purified goat anti-rat IgG antibodies (ZYMED Laboratories) was used for this assay. Color reaction was revealed by peroxidase substrate DAB kit (DAKO). After PECAM staining, hearts or embryos were photographed and analyzed. Some samples were paraffin embedded and sectioned. Sectioned samples were dewaxed, rehydrated and mounted.

Characterization of ETS-1 mutant mice

As previously reported, the gene encoding the ETS-1 transcription factor was targeted by replacement of exon 3 and part of exon 4 with a neomycin cassette (10,11). This allele was originally described as a null allele. We subsequently demonstrated that there is splicing around the neomycin cassette to join exon 2 to exon 5 (12). Because exons 2 and 5 are in the same reading frame, the resulting mRNA is translated into a protein product that lacks sequences encoded by exons 3 and 4. Indeed, a small amount (approximately 1–2% of endogenous levels) of an internally deleted ETS-1 protein is detected in thymocyte extracts from mutant mice. The region deleted encodes the pointed domain of ETS-1, which is involved in protein–protein interactions with the Erk kinase and with CBP/p300. These interactions are important for maximal trans-activation of ETS-1 target genes (13,14). Thus, any protein product from the targeted allele is likely to be defective in its trans-activation properties and is most likely a functional null (10). The mice were bred into a C57/B6 genetic background, backcrossed at least 10 generations.

Embryo dissection and histological analysis

Females with copulation plugs were considered to be at embryonic development day 0.5 (E0.5) of gestation. Pregnant females were euthanized at different stages of gestation, and embryos were dissected for histological analysis as described previously (38).

LacZ staining

Wnt1-Cre; ROSA26 LacZ embryos (36) were harvested in cold PBS and fixed for 1–2 h in 4% paraformaldehyde. Embryos were subsequently incubated in beta-galactosidase substrate. For high-resolution analysis of beta-galactosidase activity, embryos were paraffin embedded and sectioned as described previously (38).

SUPPLEMENTARY MATERIAL

Supplementary Material is available at *HMG* online.

ACKNOWLEDGEMENTS

The authors would like to thank Dr Sylvia Evans for her helpful discussions and critical review of the manuscript, as well as all of the 11q- patients and their families for their unwavering support.

Conflict of Interest Statement. The authors have no conflicts of interest.

FUNDING

This work was supported by NIH KO8 HL070640-03 (P.G.), the State of South Dakota 2010 (M.Y., B.P.), The Carson Foundation (C.C., D.I.), NIH/NHLBI SCCOR P50 HL084923 (C.C., D.I.), NIH/NHLBI R01 HL74094 (E.G.) and by the Children's Heart Institute Fund of Rady Children's Hospital of San Diego.

REFERENCES

- Jacobsen, P., Hauge, M., Henningsen, K., Hobolth, N., Mikkelsen, M. and Philip, J. (1973) An (11;21) translocation in four generations with chromosome 11 abnormalities in the offspring. *Hum. Hered.*, **2**, 568–585.
- Penny, L.A., Dell'Aquila, M., Jones, M.C., Bergoffen, J., Cunniff, C., Fryns, J.P., Grace, E., Graham, J.M. Jr, Kousseff, B., Mattina, T. *et al.* (1995) Clinical and molecular characterization of patients with distal 11q deletions. *Am. J. Hum. Genet.*, **56**, 676–683.
- Tunnacliffe, A., Jones, C., Le Paslier, D., Todd, R., Cherif, D., Birdsall, M., Devenish, L., Yousry, C., Cotter, F.E. and James, M.R. (1999) Localization of Jacobsen syndrome breakpoints on a 40Mb. physical map of distal chromosome 11q. *Genome Res.*, **9**, 44–52.
- Grossfeld, P.D., Mattina, T., Lai, Z., Favier, R., Jones, K.L., Cotter, F. and Jones, C. (2004) The 11q terminal deletion disorder: a prospective study of 110 cases. *Am. J. Med. Genet.*, **15**, 51–61.
- Oikawa, T. and Yamada, T. (2003) Molecular biology of the Ets family of transcription factors. *Gene*, **16**, 11–34 (Review).
- Bartel, F.O., Higuchi, T. and Spyropoulos, D.D. (2000) Mouse models in the study of the Ets family of transcription factors. *Oncogene*, **19**, 6443–6454.
- Remy, P. and Baltzinger, M. (2000) The Ets-transcription factor family in embryonic development: lessons from the amphibian and bird. *Oncogene*, **19**, 6417–6431.
- Bories, J.C., Willerford, D.M., Grévin, D., Davidson, L., Camus, A., Martin, P., Stéhelin, D. and Alt, F.W. (1995) Increased T-cell apoptosis and terminal B-cell differentiation induced by inactivation of the Ets-1 proto-oncogene. *Nature*, **377**, 635–638.
- Eyquem, S., Chemin, K., Fasseu, M. and Bories, J.C. (2004) The Ets-1 transcription factor is required for complete pre-T cell receptor function and allelic exclusion at the T cell receptor beta locus. *Proc. Natl Acad. Sci. USA*, **101**, 15712–15717.

10. Muthusamy, N., Barton, K. and Leiden, J.M. (1995) Defective activation and survival of T cells lacking the Ets-1 transcription factor. *Nature.*, **377**, 639–642.
11. Barton, K., Muthusamy, N., Fischer, C., Ting, C.N., Walunas, T.L., Lanier, L.L. and Leiden, J.M. (1998) The Ets-1 transcription factor is required for the development of natural killer cells in mice. *Immunity*, **9**, 555–563.
12. Wang, D., John, S.A., Clements, J.L., Percy, D.H., Barton, K.P. and Garrett-Sinha, L.A. (2005) Ets-1 deficiency leads to altered B cell differentiation, hyperresponsiveness to TLR9 and autoimmune disease. *Int. Immunol.*, **17**, 1179–1191.
13. Seidel, J.J. and Graves, B.J. (2002) An ERK2 docking site in the Pointed domain distinguishes a subset of ETS transcription factors. *Genes. Dev.*, **16**, 127–137.
14. Foulds, C.E., Nelson, M.L., Blaszczyk, A.G. and Graves, B.J. (2004) Ras/mitogen-activated protein kinase signaling activates Ets-1 and Ets-2 by CBP/p300 recruitment. *Mol. Cell. Biol.*, **24**, 10954–10964.
15. Sato, Y. (2001) Role of ETS family transcription factors in vascular development and angiogenesis. *Cell Struct. Funct.*, **26**, 19–24.
16. Zhan, Y., Brown, C., Maynard, E., Anshelevich, A., Ni, W., Ho, I.C. and Oettgen, P. (2005) Ets-1 is a critical regulator of Ang II-mediated vascular inflammation and remodeling. *J. Clin. Invest.*, **115**, 2508–2516.
17. Davidson, B., Shi, W., Beh, J., Christiaen, L. and Levine, M. (2006) FGF signaling delineates the cardiac progenitor field in the simple chordate, *Ciona intestinalis*. *Genes Dev.*, **20**, 2728–2738.
18. Alvarez, A.D., Shi, W., Wilson, B.A. and Skeath, J.B. (2003) Pannier and pointedP2 act sequentially to regulate Drosophila heart development. *Development*, **130**, 3015–3026.
19. Lie-Venema, H., Gittenberger-de Groot, A.C., van Empel, L.J., Boot, M.J., Kerkdijk, H., de Kant, E. and DeRuiter, M.C. (2003) Ets-1 and Ets-2 transcription factors are essential for normal coronary and myocardial development in chicken embryos. *Circ. Res.*, **92**, 749–756.
20. Hart, A., Melet, F., Grossfeld, P., Chien, K., Jones, C., Tunnacliffe, A., Favier, R. and Bernstein, A. (2000) Fli-1 is required for murine vascular and megakaryocytic development and is hemizygotously deleted in patients with thrombocytopenia. *Immunity*, **13**, 167–177.
21. Spyropoulos, D.D., Pharr, P.N., Lavenburg, K.R., Jackers, P., Papas, T.S., Ogawa, M. and Watson, D.K. (2000) Hemorrhage, impaired hematopoiesis, and lethality in mouse embryos carrying a targeted disruption of the Fli1 transcription factor. *Mol. Cell Biol.*, **20**, 5643–5652.
22. Wickman, K., Nemecek, J., Gendler, S.J. and Clapham, D.E. (1998) Abnormal heart rate regulation in GIRK4 knockout mice. *Neuron*, **20**, 103–114.
23. Simon, D.B., Karet, F.E., Rodriguez-Soriano, J., Hamdan, J.H., DiPietro, A., Trachtman, H., Sanjad, S.A. and Lifton, R.P. (1996) Genetic heterogeneity of Bartter's syndrome revealed by mutations in the K⁺ channel, ROMK. *Nat. Genet.*, **14**, 152–156.
24. Nasu-Nishimura, Y., Hayashi, T., Ohishi, T., Okabe, T., Ohwada, S., Hasegawa, Y., Senda, T., Toyoshima, C., Nakamura, T. and Akiyama, T. (2006) Role of the Rho GTPase-activating protein RICS in neurite outgrowth. *Genes Cells*, **11**, 607–614.
25. Maroulakous, I.G., Papas, T.S. and Green, J.E. (1994) Differential expression of ets-1 and ets-2 proto-oncogenes during murine embryogenesis. *Oncogene*, **9**, 1551–1565.
26. Jiang, X., Rowitch, D.H., Soriano, P., McMahon, A.P. and Sucov, H.M. (2000) Fate of the mammalian cardiac neural crest. *Development*, **127**, 1607–1616.
27. Tyson, C., Qiao, Y., Harvard, C., Liu, X., Bernier, F.P., McGillivray, B., Farrell, S.A., Arbour, L., Chudley, A.E., Clarke, L. *et al.* (2008) Submicroscopic deletions of 11q24-25 in individuals without Jacobsen syndrome: re-examination of the critical region by high-resolution array-CGH. *Mol. Cytogenet.*, **1**, 23.
28. Wenger, S.L., Grossfeld, P.D., Siu, B.L., Coad, J.E., Keller, F.G. and Hummel, M. (2006) Molecular characterization of an 11q interstitial deletion in a patient with the clinical features of Jacobsen syndrome. *Am. J. Med. Genet. A*, **140**, 704–708.
29. Bernaciak, J., Szczaluba, K., Derwinska, K., Wisniewiecka-Kowalnik, B., Bocian, E., Sasiadek, M.M., Makowska, I., Stankiewicz, P. and Smigiel, R. (2008) Clinical and molecular-cytogenetic evaluation of a family with partial Jacobsen syndrome without thrombocytopenia caused by an approximately 5 Mb deletion del(11)(q24.3). *Am. J. Med. Genet. A*, **146A**, 2449–2454.
30. Phillips, H.M., Renforth, G.L., Spalluto, C., Hearn, T., Curtis, A.R., Craven, L., Havarani, B., Clement-Jones, M., English, C., Stumper, O. *et al.* (2002) Narrowing the critical region within 11q24-qter for hypoplastic left heart and identification of a candidate gene, JAM3, expressed during cardiogenesis. *Genomics*, **79**, 475–478.
31. Ye, M., Geddis, A., Perryman, M.B. and Grossfeld, P.D. (2009) Deletion of JAM-C, a candidate gene for heart defects in Jacobsen syndrome, results in a normal cardiac phenotype. *Am. J. Med. Genet. A*, **149A**, 1438–1443.
32. Moscoso, G. and Pexieder, T. (1990) Variations in microscopic anatomy and ultrastructure of human embryonic hearts subjected to three different modes of fixation. *Pathol. Res. Pract.*, **186**, 768–774.
33. Sedmera, D., Misek, I., Klima, M. and Thompson, R.P. (2003) Heart development in the spotted dolphin (*Stenella attenuata*). *Anat. Rec. A Discov. Mol. Cell Evol. Biol.*, **273**, 687–699.
34. High, F.A., Zhang, M., Proweller, A., Tu, L., Parmacek, M.S., Pear, W.S. and Epstein, J.A. (2007) An essential role for Notch in neural crest during cardiovascular development and smooth muscle differentiation. *J. Clin. Invest.*, **117**, 353–363.
35. Hornyak, T.J., Hayes, D.J., Chiu, L.Y. and Ziff, E.B. (2001) Transcription factors in melanocyte development: distinct roles for Pax-3 and Mitf. *Mech. Dev.*, **101**, 47–59.
36. Coldren, C.D., Lai, Z., Shragg, P., Rossi, E., Glidewell, S.C., Zuffardi, O., Mattina, T., Ivy, D.D., Curfs, L.M., Mattson, S.N. *et al.* (2009) Comparative genomic hybridization mapping suggests a role for BSX and Neurogranin in neurocognitive and behavioral defects in the 11q terminal deletion disorder (Jacobsen syndrome). *Neurogenetics*, **10**, 89–95.
37. Liang, X., Sun, Y., Schneider, J., Ding, J.H., Cheng, H., Ye, M., Bhattacharya, S., Rearden, A., Evans, S. and Chen, J. (2007) Pinch1 is required for normal development of cranial and cardiac neural crest-derived structures. *Circ. Res.*, **100**, 527–535.
38. Danielian, P., Echelard, Y., Vassileva, G. and McMahon, A. (1997) A 5.5-kb Enhancer is both necessary and sufficient for regulation of Wnt-1 transcription *in vivo*. *Dev. Biol.*, **192**, 300–309.